Electronic structure of insulating zirconium nitride

P. Prieto, L. Galán, and J. M. Sanz

Departamento Física Aplicada C-XII, Universidad Autónoma de Madrid, Cantoblanco, E-28049 Madrid, Spain

(Received 24 July 1992)

The electronic structure of Zr_3N_4, grown by low-energy (0.25 keV) N_2^+ implantation of polycrystalline zirconium has been investigated by x-ray photoelectron spectroscopy. Both the valence-band and core-level spectra demonstrate the insulating characteristics of Zr_3N_4 as well as the metal-insulator phase transition in ZrN_x when $x \approx 1.33$.

In this paper we report experimental data on the electronic structure and the chemical bonding of insulating zirconium nitride (Zr_3N_4), as determined by valence-band and core-level x-ray photoelectron spectroscopy (XPS). Nitrogen-rich zirconium nitrides with a higher nitrogen content than in ZrN, have been recently obtained by using low-energy ion beams.[1,2] Furthermore, it was shown that as the nitrogen content of ZrN_x exceeds $x > 1.2$, a new optically transparent and electrically insulating phase appears to form.[1] This metastable phase has been reported for zirconium and hafnium but not for titanium and, since the composition is close to an atomic ratio of 3/4, it has been denoted as Zr_3N_4 (Hf_3N_4), suggesting a contribution of all the four valence electrons of the metal to the valence band of the compound.[1,3-5]

A Josephson junction built with superconductor ZrN and insulator Zr_3N_4 has been proposed,[3] since these materials are related chemically and structurally and would have a perfect match at the interface.

The electronic structure of ZrN_x for the entire substoichiometric range associated with the rocksalt structure (i.e., $0.5 \leq x \leq 1$) has been extensively studied both theoretically and experimentally.[6-9] Although the insulating properties of Zr_3N_4 are obviously related to its electronic structure, it appears that electron spectroscopic studies of that phase have not been published. Therefore, the XPS study we present in this paper seems well motivated.

Polycrystalline Zr 25 μm thick has been used in this work. After cleaning the surface by Ar^+ sputtering and annealing at 1300 K, zirconium nitrides ZrN_x were obtained by low-energy (2.00 and 0.25 keV) N_2^+ implantation in a preparation chamber attached to the spectrometer. The ion source was of the Penning type producing a nitrogen ion current of ≈ 5 μA on an area of ≈ 5 cm^2. In addition, thermally grown ZrN samples were obtained by annealing the Zr foil at 1400 K in NH_3 atmosphere $(P_{NH3} = 4 \times 10^{-4}$ Torr).

XPS spectra were recorded in a commercial LHS-10 spectrometer from Leybold using Mg K_α radiation as an excitation source. Mg $K_{\alpha,3,4}$ radiation satellites were numerically subtracted. The analyzer was operated in the constant-pass energy mode $(E_{pass} = 20$ eV) with an energy resolution of ≈ 0.3 eV.

Figure 1 shows the XPS valence-band spectra recorded

for two different nitrides with average compositions $ZrN_{1.3}$ and $ZrN_{1.0}$ (as determined by quantitative XPS) obtained by N_2^+ implantation at 250 eV and 2 keV, respectively. For comparison, the valence band for metallic Zr has also been depicted. The spectra have been normalized to the intensity of the corresponding Zr 3d line, so that they represent the valence-band density of states per Zr atom modulated by the respective photoionization cross sections of the levels involved. The difference spectrum ZrN-Zr_3N_4 has also been included in Fig. 1 to emphasize the differences between both nitrides.

With reference to the valence-band spectra of the nitrides, previous experimental and theoretical data for ZrN (Refs. 6–9) allow one to identify the large emission band at 6 eV below the Fermi energy as due to N 2p states strongly hybridized to Zr 4d states and the structure near the Fermi level as a nearly pure-metal Zr 4d
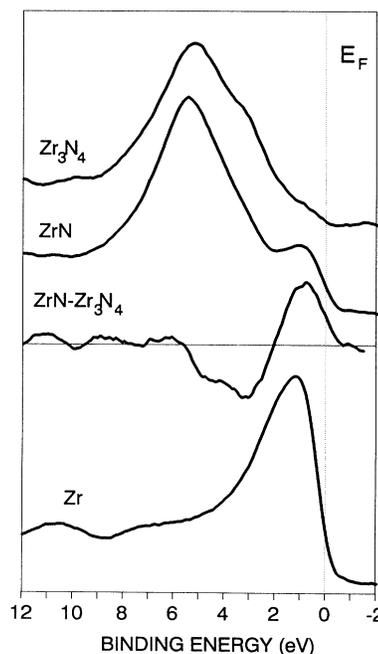
FIG. 1. Valence-band photoemission spectra of Zr_3N_4, ZrN, and Zr (as labeled) normalized to the intensity of the respective Zr 3d core lines, and ZrN-Zr_3N_4 difference spectrum.

band weakly mixed with N $2p$ states. In fact, the intensity of this d-like band between 0 and 2.5 eV has been observed to decrease when x (ZrN$_x$) increased from 0.5 to 1.[8] However, no results existed for nitrogen-rich nitrides (i.e., $x > 1$). Figure 1 clearly shows that for ZrN$_{1.3}$ the emission band just below E_F is almost completely depopulated and the nitride transforms from metallic to insulating, in agreement with results obtained from optical and conductivity measurements.[1] A simple quantification of such a band by fitting it to the valence band of metallic Zr gives a density of electrons per atom of Zr of $n_d = 0.97$ for ZrN$_{1.0}$ and 0.3 for ZrN$_{1.3}$. A more complete analysis including other ZrN$_x$ samples over a wide range of compositions (i.e., $0 \le x \le 1$) (Ref. 10) shows that n_d depends linearly on x according to $n_d = (4 - 3x) \pm 0.08$ which gives $n_d = 0$ for $x = 1.33$ (i.e., Zr$_3$N$_4$).

With respect to the valence band of ZrN, the band structure of ZrN$_{1.3}$ appears also affected around 4 eV. This is also observed in the difference spectrum (i.e., ZrN-Zr$_3$N$_4$), where a double structure can be easily distinguished. According to our experience,[10] that shoulder at ≈ 4 eV is closely related to the use of low-energy N$_2^+$ ions. It appears to increase with composition x and becomes quite significant for ZrN$_{1.3}$. In any case, it disappears upon annealing at 1000 K. The difference spectrum of Fig. 1 suggest that electrons near E_F are being transferred to the new states at 3.5 and 4.8 eV, so that the nitride becomes an insulator. The data provide a visualization of the emptying of the conduction band of ZrN and the opening of a gap of ≈ 2 eV. In fact, existing band-structure calculations and angle-resolved-photoemission measurements[7,9] suggest that emission at that energy is associated with a band of Δ_5 symmetry at ≈ 3.5 eV whose electronic structure can be described as pd_π bands between the N p and Zr d orbitals (of t_{2g} symmetry) which has an important ionic component.[7,9,11]

According to that, we are observing an increased hybridization and a stronger localization of the Zr d electrons. Consequently, there is a larger charge transfer from Zr to N and the bonding becomes more ionic. The effect of such charge transfer in the core-level binding energies will be discussed below.

The structure of Zr$_3$N$_4$ is not known in detail. Schwarz et al.[3] proposed a highly defective NaCl structure with Zr vacancies. The same authors also realized an augmented spherical-wave band-structure calculation considering two different nitrogen sites, depending on whether they were coordinated by four or six zirconium atoms. Although they showed a significant lowering of the electron density at E_F as compared with ZrN, the calculations still yield conduction. Probably, as the same authors suggest, the occurrence of the insulating phase is related to some kind of structure metastable with a coordination of five for the nitrogen atoms.[3] In fact, it appears that this metastable phase is mainly obtained by methods assisted by ion beams, whereby bombardment by energetic N$_2^+$ ions increases the incorporation of nitrogen in the solid, so that films with nitrogen in excess can form in response to an abundant N$_2^+$ flux.

We turn now to the analysis of the Zr $3d$ and N $1s$

TABLE I. Range of compositions x, Zr $3d$ binding energies relative to the clean metal [ΔE_B(Zr $3d$)], N $1s$ binding energy [E_B (N $1s$)], and differences in binding energies [ΔE_B(Zr $3d$-N $1s$)] for the three phases α-Zr, ZrN, and Zr$_3$N$_4$. The error in composition is ± 0.05 and in energy is ± 0.05 eV.

	ZrN$_x$ x range	ΔE_B(Zr $3d$) (eV)	E_B(N $1s$) (eV)	ΔE_B(Zr $3d$-N $1s$) (eV)
α-Zr	0–0.25	0–0.25	397.3	−218.30 to −218.05
ZrN	0.7–1.00	0.6–1.3	397.3	−217.70 to −217.00
Zr$_3$N$_4$	1.3	2.0	396.4	−215.4

core-level spectra, which also provide interesting information. The experimental data are shown in Fig. 2 for ZrN$_{1.3}$ and ZrN obtained by N$_2^+$ implantation at 0.25 and 2 keV, respectively, as well as for a ZrN thermally grown in NH$_3$ atmosphere and for Zr metal. The results of the line-shape fitting are also shown for both Zr $3d$ and N $1s$ of every compound, showing that except for ZrN obtained by implantation at 2 keV, where a small amount of a second phase (i.e., Zr$_3$N$_4$) can be distinguished in both the Zr $3d$ and N $1s$, the other spectra correspond well to single-phase compounds. For Zr$_3$N$_4$ the N $1s$ spectrum also shows a second peak at ≈ 398 eV, which is
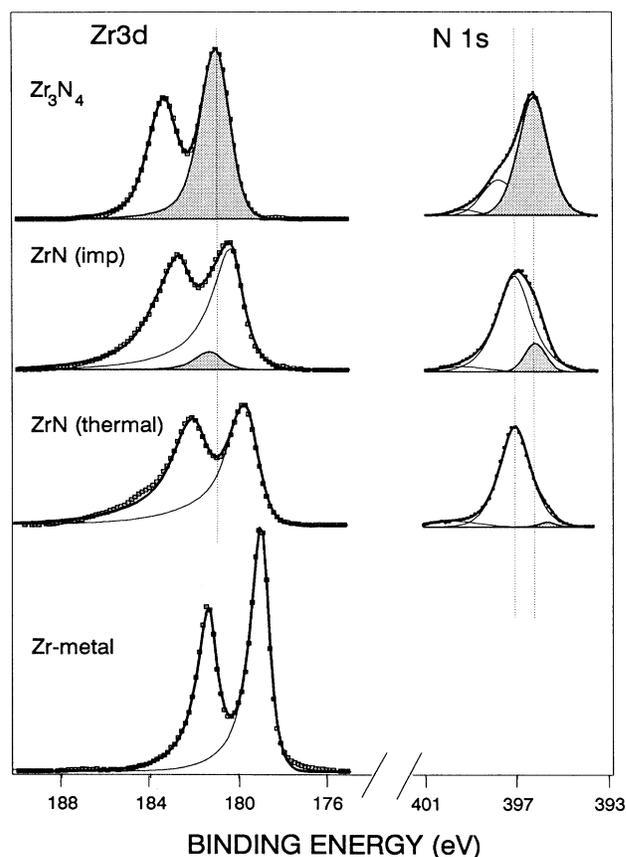
FIG. 2. Least-squares analysis of the Zr $3d$ and N $1s$ XPS lines of Zr$_3$N$_4$, ZrN obtained by N$_2^+$ implantation, ZrN obtained by annealing in NH$_3$, and clean Zr (see Table II and text). The shadowed peaks correspond to the Zr$_3$N$_4$ phase.

assigned to adsorbed nitrogen and accounts for about 0.4 surface monolayers. In fact, all the ZrN_x samples we have studied, over the entire composition range (i.e., $0 \le x \le 1.3$) could be fitted in terms of the spectra for metallic Zr with some dissolved nitrogen (i.e, α-Zr), ZrN, and Zr_3N_4.[10] The corresponding x range of existence, as well as the energy position of the Zr 3d levels relative to the metal, the N 1s binding energy, and the Zr 3d-N 1s binding-energy difference, are given in Table I. With respect to the metal, the Zr 3d-level shifts between 0.6 and 1.3 eV for the ZrN $(0.7 \le x \le 1)$ are in good agreement with previous reports,[6-8] whereas N 1s remains at 397.3 eV over the whole compositional range. On the contrary, when the stoichiometry reaches Zr_3N_4, both the Zr 3d and N 1s undergo significant shifts in opposite directions (i.e., 0.7 and -0.9 eV with respect to ZrN), increasing significantly the N 1s–Zr 3d binding-energy difference (cf. Table I). All that is a clear indication of the electronic changes and charge transfer from Zr to N, which occur when the stoichiometry is changed from ZrN to $ZrN_{1.3}$, so that the bond becomes more ionic, the charge is more strongly localized, and $ZrN_{1.3}$ becomes an insulator. The shape of the Zr 3d core lines also supports the above-mentioned changes in electronic structure and bonding properties. The peaks were well fitted in terms of Doniach-Sunjic functions[12,13] convoluted with the analyzer resolution function (full width at half maximum equals 0.3 eV) and the spectrum of the excitation source (i.e., Mg K_α). An examination of Fig. 2 shows that there is a long tail toward higher binding energies in the case of ZrN. This tail, although not so pronounced , is also present in the case of the metal but it is barely observable for Zr_3N_4. In fact, the asymmetry parameter α deduced from the analysis of the spectra (cf. Table II) is 0.15 for Zr, 0.3 for ZrN, and 0.005 for Zr_3N_4. According to Doniach and Sunjic,[12] the tail of the lines (i.e., α) is closely related to the coupling of the core hole with the electrons at the Fermi level. Therefore, the observed in-

TABLE II. Best-fit parameters for the line shapes of the Zr 3d XPS spectra of Zr, ZrN, and $ZrN_{1.3}$

	Gaussian width (eV)	Lorentzian width (eV)	α
Zr	0.39	0.45	0.15
ZrN	0.74	0.52	0.30
$ZrN_{1.3}$	1.17	0.45	0.05

creased of α from Zr to ZrN is just an indication of the enhanced conductivity of ZrN with respect to the metal, as well as a higher valence-electron density, and of a more effective screening of the 3d hole by the conduction band of ZrN with increased p character. However, from the absence of asymmetric broadening in the case of Zr_3N_4 one concludes that the density of conduction electrons vanishes and, therefore, the coupling is much weaker, which is in agreement with the observed enhancement of the localization of the valence electrons and the opening of a band gap at the Fermi level.[13,14] Furthermore, Table II clearly shows that whereas the Lorentzian contribution to the line (i.e., the intrinsic width of the core hole) is almost the same for the three compounds, the Gaussian contribution increases noticeably for Zr_3N_4 as expected for an enhancement of polarity of the bond in going from Zr to Zr_3N_4.

In conclusion, we have reported and analyzed XPS valence-band and core-level spectra of Zr_3N_4, which clearly demonstrates its insulating properties, as well as the polar character of its bonding in comparison with metallic ZrN. In fact, the results show a metal-to-insulator phase transition in ZrN_x when x reaches a value close to 1.33.

[1]B. O. Johansson, H. T. G. Hentzell, J. M. E. Harper, and J. J. Cuomo, J. Mat. Res. 1, 442 (1986).

[2]B. O. Johansson, J. E. Sundgren, U. Helmersson, and M. -K. Hibbs, Appl. Phys. Lett. 44, 670 (1984).

[3]K. Schwarz, A. R. Williams, J. J. Cuomo, and J. M. E. Harper, Phys. Rev. B 32, 8312 (1985).

[4]K. Salmenoja, A. S. Korhonen, E. Erola, and J. M. Molarius, Appl. Phys. Lett. 49, 505 (1986).

[5]E. O. Ristolainen, J. M. Molarius, A. S. Korhonen, and V. K. Lindroos, J. Vac. Sci. Technol. A 5, 2184 (1987).

[6]H. Höchst, R. D. Bringans, P. Steiner, and Th. Wolf, Phys. Rev. B 25, 7183 (1982).

[7]A. Callenas, L. I. Johansson, A. N. Christensen, K. Schwarz, P. Blaha, and J. Redinger, Phys. Rev. B 30, 635 (1984).

[8]L. Porte, Solid State Commun. 50, 303 (1984).

[9]J. Lindström, L. I. Johansson, A. Callenas, D. S. L. Law, and A. N. Christensen, Phys. Rev. B 35, 7891 (1987).

[10]P. Prieto (unpublished); P. Prieto, Ph.D. thesis, Universidad Autonoma de Madrid (1992).

[11]A. Neckel, P. Rastl, R. Eibler, P. Weinberger, and K. Schwarz, J. Phys. C 9, 579 (1976).

[12]S. Doniach and M. Sunjic, J. Phys. C 3, 285 (1970).

[13]G. K. Wertheim and P. H. Citrin, in Photoemission in Solid I, edited by M. Cardona and L. Ley, Topics in Applied Physics Vol. 26 (Springer, Berlin, 1978).

[14]M. Campagna, G. K. Wertheim, H. R. Shanks, F. Zumsteg, and E. Banks, Phys. Rev. Lett. 34, 738 (1975).